https://doi.org/10.15407/ufm.24.04.792

A.T. TURDALIEV [1], M.A. LATYPOVA [2,*], and E.N. RESHOTKINA [3,]**

[1] International Transport and Humanitarian University,
32 Zhetisu 1 Microdistrict, 050063 Almaty, Kazakhstan

[2] Karaganda Industrial University,
30 Republic Ave., 101400 Temirtau, Kazakhstan

[3] 'ArcelorMittal Temirtau' Corporation,
1 Republic Ave., 101400 Temirtau, Kazakhstan

* m.latypova@tttu.edu.kz, ** elena.reshotkina@arcelormittal.com

SYNTHETIC-HYDROXYAPATITE-BASED COATINGS ON THE ULTRAFINE-GRAINED TITANIUM AND ZIRCONIUM SURFACE

The development of biocompatible materials is a multidisciplinary task and requires the interaction of physicists, chemists, biologists, and physicians, since the functional reliability of materials depends on their biochemical, cellular, tissue, and biomechanical compatibility. This area has been developing intensively in recent years, resulting in numerous research articles. As assumed, the composition of the biocompatible coating of the new generation should coincide as much as possible with the composition of natural human bone and be able to simulate bone tissue on its surface. As a result of the approximation of the phase-structural state and properties of the resulting coatings on implants to the parameters of bone tissue, improved compatibility between them can be achieved. When forming biocompatible coatings, special attention is paid to creating a definite relief (roughness) on the implant surface. There is a current search for new technological solutions for creating a biocompatible rough surface on implants that ensures reliable integration of the implant into bone tissue, since existing technologies do not fully meet state-of-the-art medical requirements.

Keywords: ultrafine-grained materials, titanium, zirconium, coating, implant.

Citation: T. Turdaliev, M.A. Latypova, and E.N. Reshotkina, Synthetic-Hydroxyapatite-Based Coatings on the Ultrafine-Grained Titanium and Zirconium Surface, *Progress in Physics of Metals*, **24**, No. 1: 792–818 (2023)

1. Introduction

Metals and alloys are widely used in medicine as material for implant manufacture in traumatology, orthopaedics, maxillofacial surgery, dentistry, *etc.* [1–9]. Since ancient times, there have been numerous attempts to use both precious metals (gold and silver) and iron alloys in various injuries treatment. Nevertheless, the comprehended use of metals became possible only in the XIX–XX centuries, when scientific biocompatibility problem approaches were developed, and the necessary technologies in metallurgy were developed [10–16].

It is known that the first orthopaedic implants were made of iron-based alloys. The mechanical and physicochemical parameters of these materials are high enough. However, they have a low level of biocompatibility and corrosion resistance in aggressive biological environments, which can cause various allergic and inflammatory reactions development, which has limited their active use. Currently, 30X13 and 40X13 steel grades are used to manufacture surgical instruments, springs, rods, plates, *etc*. For the manufacture of spokes, staples, and clamps in external fixation devices for the treatment of bone fractures, more plastic steel of the 12X18N10T brand is used [17–19].

Steel 12X18N10T has increased resistance to intercrystalline corrosion due to the formation of sufficiently large carbide particles after high tempering and quenching in oil. Today, steel is a material with a good combination of strength, plasticity and with a relatively low cost. However, steel and steel alloys are inferior in biocompatibility to metals and alloys based on titanium, zirconium, niobium, and tantalum.

The next stage in the development of medical materials science was the use of cobalt–chromium–molybdenum alloys containing up to 25–30% chromium, 5–7% molybdenum and a small number of other metals for the manufacture of metal orthopaedic implants [20].

Chromium–cobalt alloy is also used to manufacture implants and the metal base of solid-cast denture structures based on implants. Even though cobalt–chromium–molybdenum and stainless steels have high mechanical characteristics, they are less and less used in orthopaedics today due to the high probability of emission of toxic alloying elements from the implant into the surrounding tissues of the body. Intensive electrochemical reactions with the formation of toxic compounds are observed on the surface of an implant made of cobalt–chromium–molybdenum alloy after its introduction into the body, which negatively affects the biocompatibility of this implant [20].

Noble metals, primarily such as gold and platinum, have a ‘clean’ metal surface, therefore, they have very high corrosion resistance and biocompatibility, but they have a high cost that also limits their use.

The most popular and commonly used metal materials in medicine are titanium and its alloys [17–19]. A large number of scientific papers

have been devoted to the study of the mechanical, chemical, and biological properties of titanium and titanium alloys [21–23]. From the point of view of chemical and electrochemical biocompatibility, titanium has several advantages over other metals used in medicine: high biocompatibility; good corrosion resistance; bio-tolerance; non-magnetism; low thermal conductivity; small coefficient of linear thermal expansion; the almost complete absence of toxic phenomena. Therefore, titanium is the most preferred metal for the manufacture of orthopaedic, traumatological and dental implants.

In addition, titanium is of great practical interest due to its relatively high physical and mechanical properties and relative availability. Titanium with a small amount of impurities that fall during metal smelting is considered technically pure or unalloyed. It should be noted that the mechanical properties of titanium, like any other metals, largely depend on the content of impurities, the technology of production, and further heat treatment and can vary significantly.

2. Ultrafine-Grained (UFG) Titanium and Its Alloys

The rapid development of nanotechnology has not spared medical implants. Currently, methods of intensive plastic deformation have been developed to obtain bulk nanostructured (NS) metallic materials, including titanium and titanium alloys. Receiving a homogeneous fine-grained structure and nanostructure in titanium made it possible to form a material with high mechanical properties corresponding to titanium alloys for medical purposes. Pure titanium does not contain alloying elements harmful to the body. At the same time, the phase and elemental composition do not change, and nanostructured titanium can be successfully applied in medical practice. Calcium-phosphate coatings (amorphous, nanocrystalline, and crystalline) are applied to the surface of titanium products, which makes it possible to give the product the necessary operational properties without changing its structure.

Titanium has been widely used in surgery since the 1950s and is the main material for the production of various implants. Technically pure titanium grades VT1-0, VT1-00, Grade 1 Grade 2 Grade 3, and Grade 4 and their alloys VT6, VT16, and titanium nickelide are used for the production of dental implants. In orthopaedics and traumatology, titanium alloys with vanadium, molybdenum, aluminium, nickel, and cobalt are used for the manufacture of implants (spokes, nails, plates, bolts, and screws for fixing damaged joints and bones), in particular, alloys VT5, VT6, VT16, *etc.* [23, 24]. Nevertheless, some researchers [25–30] express concerns about using titanium alloys for implant manufacture due to the likelihood of the alloying elements released on the implant surface, which can lead to the intoxication of the surrounding tissues.

Thus, the composition of the VT6 alloy includes aluminium, vanadium, and molybdenum, which in themselves are toxic and, if ingested into living tissues, can lead to undesirable processes in the body.

In modern medical practice, implants made of titanium or titanium alloys are widely used to replace damaged or defective tissue areas. However, implant usage with a significant difference in the physicochemical and mechanical properties of bone tissue and alloy causes active rejection in the human body and, as a consequence, further complications in treatment. It is necessary to create a transition zone between the implant and the bone, which can have a strong connection with the implant material, as well as a macro and microstructure acceptable to the body, to reduce the negative impact of such factors. Such a zone should be obtained in the coating form having a developed morphology and a definite porosity for more effective implant engraftment.

The biocompatibility of titanium and its alloys is mainly due to the spontaneous formation of an inert oxide layer on their surface [31, 32]. Titanium is a reactive metal that, when exposed to oxygen, is rapidly oxidized (within milliseconds), which leads to the formation of an oxide nanolayer of almost stoichiometric TiO_2 of 1–10 nm thickness on its surface, preventing further oxidation of the metal. The nanolayer is loosely connected to the substrate and can be damaged even with weak mechanical action. That happens during the manufacture of the implant, during its installation, as well as during operation. It is especially actively destroyed under the influence of cyclic loads in the biological environments of the body. This process is called 'fretting corrosion'. To prevent this process, there are methods for the artificial formation of an oxide or nitride layer on the surface of titanium, which is firmly bound to the base and has corrosion and mechanical resistance [33].

At the same time, the main disadvantage and limiting factor for expanding the range of titanium applications in dental implantology, dentistry, maxillofacial surgery, and traumatology is the low level of mechanical properties of pure titanium. The problem of increasing the mechanical strength of titanium has been successfully solved due to its conversion by methods of intensive plastic deformation into an ultrafine-grained and nanostructured state [34].

To date, numerous studies by research teams from around the world have substantiated the prospect of radically improving the mechanical properties of metals and alloys, including titanium, due to the formation of a nanoscale structure. In recent years, intensive plastic deformation (IPD) methods have been actively developed, which make it possible to obtain volumetric ultrafine-grained and metallic materials with unique physical and mechanical properties [35–45]. Scientific work on this topic is carried out in collectives and centres in several laboratories in the USA, France, Japan, Germany, Russian Federation, *etc*. Scien-

tific and practical interest in the ultrafine-grained materials development is confirmed by the development of a new scientific direction, which is considered the basis for the creation of metals and alloys of the next generation [46–50].

There are a vast number of publications, in which it is shown that the use of various IPD methods makes it possible to form nanostructured and ultrafine-grained states in pure metals, alloys, and steels in the material [35–54]. At the same time, a large number of works are devoted to titanium and alloys based on it, in which it is shown that the mechanical properties of ultrafine-grained (nanostructured) titanium correspond to medium-alloyed titanium alloys (VT6, VT16) and can replace them.

Using ultrafine-grained (nanostructured) titanium in medicine makes it possible to exclude the negative effect of alloying additives in titanium alloys, such as aluminium, vanadium, and molybdenum, on a living organism [51–54].

The formation of UFG structures in titanium alloys by IPD methods is possible only at elevated temperatures due to the low deformation ability of these materials. In Ref. [52], multistep isothermal all-round forging of Ti–6Al–4V alloy was carried out with a decrease in temperature in the range of 800–450 °C. The influence of various types of the initial structure of the Ti–6Al–4V alloy: martensitic after quenching at 1010 °C, globular $\alpha + \beta$ structure (isothermal forging at 700 °C), mixed structure (isothermal forging at 950 °C followed by air cooling), on forging parameters and grinding is investigated in Ref. [53]. The authors have shown that compression of alloy blanks with martensitic and globular structures by 70% at 550 °C leads to homogeneous grain structure formation, the average size of the elements of which was less than 1 micron. In the case of the initial bimodal structure, only the lamellar component of the α-phase transformed grains, while the large grains of the primary α-phase were oriented in the direction of the material flow. It was shown that the all-round forging method of Ti–6Al–4V alloy along three orthogonal directions leads to homogeneous structure formation with a grain size of 0.3 microns. The authors call the formation process of high-angle transverse boundaries in phase plates' dynamic recrystallization by a continuous mechanism. The authors [53] also note that the evolution of the plate structure of the alloy into a globular one during all-round forging strongly depends on the initial orientation of the plates of the α-phase. With a favourable orientation of the plate colonies relative to the compression axis (c axis is between 15° and 75°), which ensures the implementation of basic and prismatic sliding, transverse small-angle boundaries are formed by accumulation and redistribution of dislocations. The deformation of the colonies of plates with a less favourable orientation (the c axis is an angle of about 20 or about

75° with the compression axis) is realized through shear deformation, while this effect increases with a decrease in temperature. The deformation shift destroys the lamellar structure and contributes to the formation of transverse intraphase boundaries with misorientation, which varies from small to high-angle. At the same time, bending the plate rotates its fragments and reduces the sliding resistance of dislocations. Thus, multistage compression during free forging with a change in the direction of deformation accelerates the globularization of the lamellar structure, since, at each step of deformation, various dislocation-sliding systems are activated [54].

In Ref. [55], the influence of the initial structure of Ti–6Al–4V alloy blanks on the structure formation in it during equal-channel angular pressing (ECAP) at temperatures of 500–700 °C was considered. Blanks with the following types of structures were pressed: (1) globular structure with an average α-grain size of 11 microns (heating at 950 °C, 2 hours, cooling in the oven); (2) lamellar with an average colony size of 300 microns and a plate thickness of 4 microns (heating at 1050 °C, 1 hour, cooling in the oven). It was shown that the minimum temperature of the IPD implementation by this method was 600 °C. At a temperature of 500 °C, the destruction of workpieces and surface defects were observed, regardless of the type of structure.

In Ref. [56], detailed studies of the microstructure of the Ti–6Al–4V alloy were carried out after 1 pass of the ECAP at 600 °C. It was found that three types of characteristic microstructures are formed in the workpiece with the initial globular structure: (a) parallel shear bands with a thickness of 0.2 microns inside the α-grains, which are formed in the plane of the basis; (b) a strongly deformed structure near the β-phase; (c) weakly deformed β-grains. The structure near the β-phase can be characterized by the formation of scattered cellular structures and equiaxed ultrafine grains with wide extinction contours. The authors suggest that these large dislocation clusters are an indicator that various sliding modes, including prismatic and pyramidal sliding, are activated during deformation, while the β-phase grains act as barriers to the movement of dislocations during ECAP.

No shear bands were found in the blank with the initial plate structure after the ECAP. The density of dislocations with basic slip is low, and small-angle boundaries are formed in the β-plates. Well-developed shear bands in the plane of the basis are observed at the boundaries of the plate colonies. According to the results of observations, it can be seen that the basic slip during ECAP is blocked not only by β-plates but also by the boundaries of colonies. The transition of the basic slip through the α/β boundary should be simple due to the crystallographic ratio compared to other systems; in this case, the colony of plates acts as a single grain for the basic slip. The initial plate structure in front of

the ECAP shows a stronger tendency to softening of the flow compared to the globular one. In previous studies, various causes of flow softening were assumed, including dislocation processes, dynamic globularization, texture, and bending of plates [57, 58]. Earlier, the authors [56] showed that the deformation of Ti–6Al–4V at 600 °C was mainly controlled by dislocation sliding processes. Since dislocations, which accumulate near the α/β boundaries are found in ECAP blanks with a globular structure, it is assumed that dislocations of an identical nature in a sample with a plate structure can accumulate in front of the plate boundaries, leading to a stress peak. After that, the transition of dislocations by sliding across the boundaries leads to the beginning of softening. Due to the stress concentration due to dislocation clusters, a lamellar structure may be undesirable compared to a globular one, where α/β boundaries may block sliding.

Thus, as follows from the analysis of the literature, there is a possibility of the formation of UFG structures in hard-to-deform low-alloyed titanium alloys by IPD methods in the field of warm deformation temperatures (0.3–0.5). These approaches can be applied to the Ti–6Al–7Nb alloy, which has not yet been studied from the point of view of the formation of UFG structures, by solving the following tasks: (1) it is necessary to choose the initial structure of the alloy to ensure its best deformation ability during SPD; (2) it is required to analyse the influence of temperature–velocity conditions and the degree of deformation on the evolution of the structure in the Ti–6Al–7Nb alloy.

3. Ultrafine-Grained Zirconium and Its Alloys

In recent years, zirconium has been used more often because of its high corrosion resistance and compatibility with human biological tissues. That made it possible to apply it in many areas of practical medicine. Replacing proven titanium with zirconium is associated with a number of distinctive advantages. Although titanium is considered as the most inert of metals, nevertheless, a few months after implantation, an increased concentration of this metal is found in the liver, kidneys, lymph nodes, and other essential organs, and a few years after implantation, its content in the contacting tissues increases more than 5 times [59].

Using implants made of steel coated with zirconium and nitrides, carbonitrides and zirconium oxycarbonitrides significantly improves the physiological condition of the injured patient in comparison with the use of similar products made of other metals. The most essential property of zirconium is its disinfecting effect.

For example, niobium-doped zirconium is biocompatible, which makes it possible to manufacture not only implants from them but also instruments for medical use. However, several medical alloys have insuffi-

ciently high strength characteristics, and in this regard, the question of improving their mechanical properties remains relevant. The use of special deformation treatments is proposed, to increase the strength characteristics, which include the methods of IPD. Zirconium-based products with higher mechanical properties can be obtained, particularly, due to the formation of an ultrafine-grained and nanostructured state over the entire volume of the workpiece. The transition to ultrafine-grained and nanostructured states significantly increases the strength properties. It is also a very urgent task to study new methods that would contribute to improving fatigue and strength characteristics. The solution to this problem is also essential for medical materials science since zirconium alloys have good biological compatibility with living tissue.

In Ref. [60], the staff of the Laboratory of Physics of Nanostructured Biocomposites of ISPMS SB $_{R}$AS, together with colleagues from the University of Duisburg-Essen (Essen, Germany) and the General Research Institute for Nonferrous Metals (Beijing, China), conducted comprehensive studies of the microstructure, mechanical and biological properties of bioinert alloys based on titanium, zirconium, and niobium in nanostructured and ultrafine-grained states. A combined method of IPD, which includes multiple *abc*-pressing (multiaxial forging) or pressing into a symmetrical channel with multipass rolling and subsequent precrystallization annealing, has been developed to obtain NS and UFG states in bulk billets made of titanium VT1-0, alloys Zr–1Nb, and Ti–45Nb. IPD method modification by replacing *abc*-pressing into a symmetrical channel makes it possible to form a nanostructure in titanium with an average size of structural elements of 100 nm. The formed UFG and NS states in titanium provide high mechanical properties comparable to medium-strength titanium alloys used in medicine. In Zr–1Nb and Ti–45Nb alloys, the combined IPD method, namely, *abc*-pressing with multi-pass rolling, obtained a UFG structure with an average size of structural elements of 200 nm, which also leads to a significant increase in the mechanical properties of the alloys, while maintaining a low modulus of elasticity commensurate with the modulus of elasticity of the cortical bone (10–40 GPa). The results of the assay of samples VT1-0, Zr1Nb, and Ti–45Nb showed good biocompatibility. Cultivation of MG63 osteosarcoma cells on samples revealed high cell viability after 10 days and good cell adhesion to the surface. UFG and NS alloys based on titanium, zirconium, and niobium are promising biomaterials for medical purposes.

4. Heat Treatment of Working Tools

When choosing the coating formation method for the implant, it is necessary to consider the scope of its application. For reconstructive surgery, calcium phosphate coatings are of interest, increasing the adhesion

strength of implants with bone tissue and enhancing their ability to osseointegration. For dentistry, maxillofacial surgery, and traumatology, biopoints that increase the strength of the attachment of implants to bone tissue are of interest. At the same time, the coatings must be stable in a biological environment and have high adhesive strength with the base material. The need for practical medicine for biocompatible coatings can be satisfied by the presence of a large range of coatings of various thicknesses, porosity, adhesive properties, *etc*. It is possible to solve this problem by using various methods of coating formation, such as plasma spraying [61–63], electrophoresis [64], sol–gel or slip method [65, 66], a biomimetic method [67, 68], magnetron sputtering and RF magnetron sputtering [69–71], a detonation-gas sputtering method [72, 73], microarc oxidation method [74, 75], *etc*.

The plasma spraying method is one of the most widely used for coatings formation, including hydroxyapatite (HA). The plasma coating process consists of feeding the coating material (in the form of a powder with defined particle sizes) using a special device into a plasma jet formed by the ionization of an inert gas stream by an electric arc, which is heated in the jet before melting is accelerated and transferred to the coated metal substrate. Upon contact with the substrate surface, the particles deform, spread, and crystallize, commonly forming agglomerates. Settling and crystallizing in layers, the particles form a coating whose properties.

Recently, there has been an increased interest in HA study as a biocompatible, resorbable material, an analogue of the mineral component of bone tissue. Studies [76, 77] have shown that titanium implants coated with hydroxyapatite, compared with implants made of pure titanium, contribute to improved ingrowth into the bone tissue of the body. In addition, biocompatible coatings on the surface of a titanium implant have a significant effect on the fixation of implants with a load, both in stable and unstable conditions [78]. Titanium implants with biocompatible coatings increase the degree of osseointegration. Such coatings prevent the penetration of titanium ions into the living tissues of the human body surrounding the implant.

HA can be synthesized using a variety of methods, which can be broadly grouped into six sets of methods: (1) dry methods including solid-phase and mechanochemical reactions [79–81]; (2) wet methods based on low-temperature chemical deposition, sol–gel method and hydrolysis [82, 83]; (3) hydrothermal methods using aqueous solutions of high temperature and high voltage, as hydrothermal, emulsion and microemulsion [84]; (4) high-temperature processes including burning [81]; (5) synthesis based on biogenic sources, which can be extracted from fish bones [85], shells [86], eggshells [87], bovine bones [88]; (6) a combination of the above methods. All methods used for the synthesis

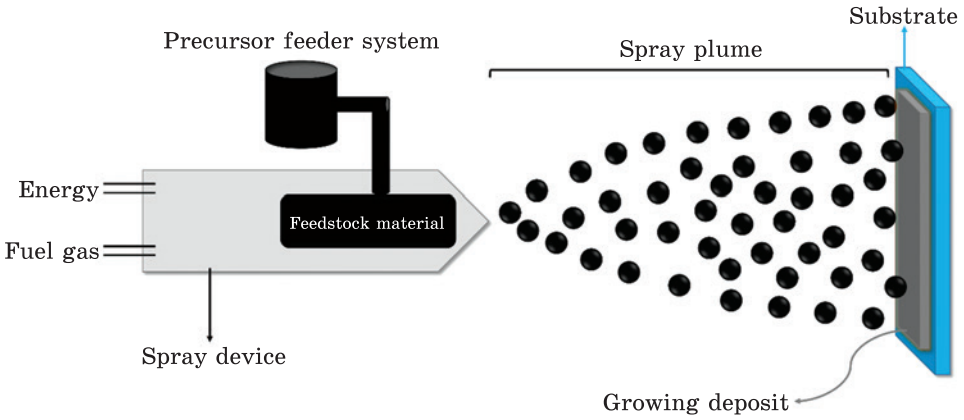

Fig. 1. Schematic representation of thermal spraying [91]

of HA particles have different technological characteristics and may have different morphology. The strength and osseointegration of powders are critical characteristics that significantly depend on their microstructure. Consequently, the main task in the synthesis of HA is to control crystal growth since its microscopic shape, size, and size distribution can significantly affect its mechanical properties, processing conditions, surface chemistry, biocompatibility, and bioactivity [89]. Thus, synthetic procedures that can precisely control the crystal geometry are of great value for expanding the potential applications of the obtained particles and nanoparticles. Obtaining HA particles with well-defined stoichiometry, high aspect ratio, and high crystallinity still has limitations. Biomedical applications require precise control of particle size and morphology, porosity, and surface area, which are fundamental characteristics that ensure reactivity and interaction with the biological system.

Let us focus on the most popular methods. Thermal spraying has found wide application in many areas of surface engineering, especially in bioceramic coatings. As a rule, this process involves high-speed spraying of molten or semi-molten particles onto a substrate, in this case, an implant, to obtain coatings up to 0.2 mm thickness. All kinds of materials, including pure metals, ceramics, alloys, and composites, can be thermally sprayed onto substrates. Thermal spraying methods can be classified depending on the heating sources used for melting the precursor [90]. The thermal spraying scheme is shown in Fig. 1.

During plasma spraying, which is carried out either in the atmosphere or in a vacuum, a constant current is established between the electrodes using a plasma-forming gas such as helium, argon, or hydrogen. These particles hit the target and are sprayed from the nozzle toward the substrate. Plasma spraying is the most commonly used thermal spraying method for applying HA coatings [92]. The thickness of

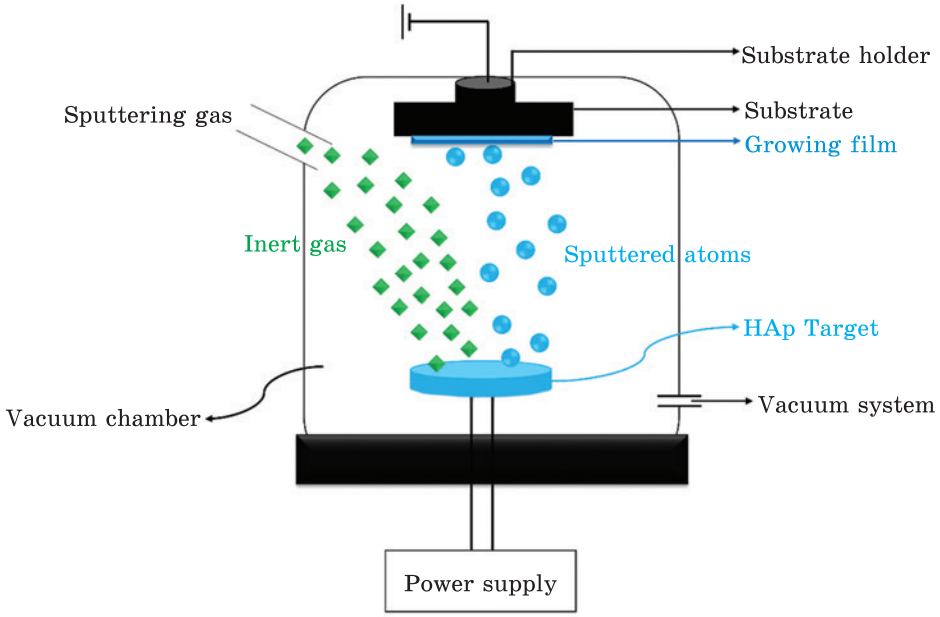

Fig. 2. PVD process diagram for HA coating [91]

hydroxyapatite (HA) coatings obtained by this method is measured in microns. For example, plasma spraying of HA coatings by Vahabzade *et al.* [80, 93] had a thickness of 150 microns, and the ones produced by Linn *et al.* [94] had a thickness of 5–50 microns.

High-speed oxygen fuel, a well-developed HA deposition method, involves burning fuel gases such as hydrogen, liquefied petroleum gas (LPG), or paraffin with oxygen to produce molten particles that can reach supersonic speeds after passing the combustion chamber to the nozzle. The type of fuel used determines the temperature of the chamber, which can vary between 2700–3100 °C [81].

Physical vapour deposition (PVD) includes many deposition processes used to manufacture thin membranes and protective coatings on electrically conductive substrates. The technique is performed in a high vacuum chamber, in which the condensed phase material (target) is converted into a vapour phase by sputtering or evaporation, followed by transferring the resulting vapour phase at the atomic level through an inert atmosphere. As a result, a condensed film is deposited on the substrate.

Recently, magnetron sputtering has attracted much attention and is rapidly developing for HA coatings. This method is often included in PVD technologies and allows to production coatings with a composition almost the same as that of the target, which provides excellent adhesion to the substrate [84]. Figure 2 shows a diagram of the PVD process for applying HA coatings.

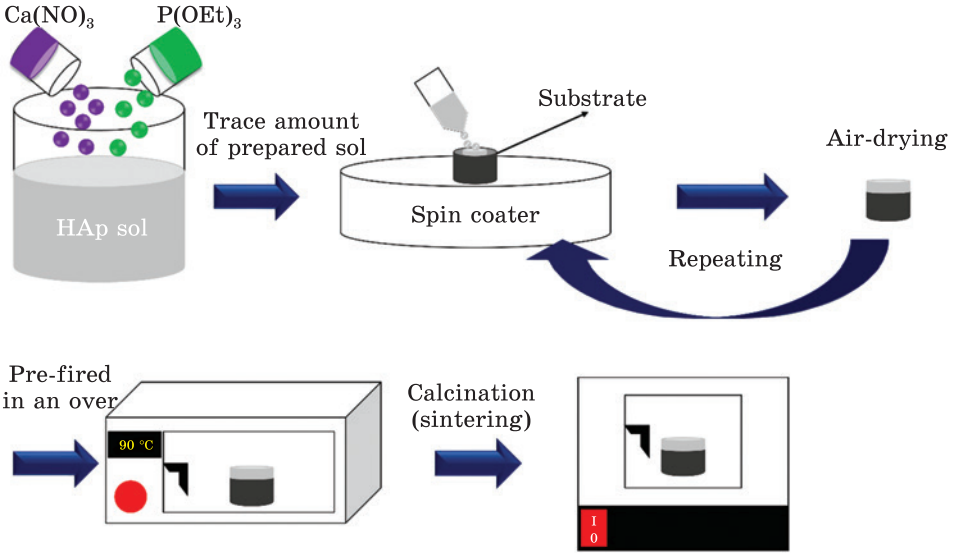

Fig. 3. Schematic representation of the centrifugation process for HA coating manufacture [91]

Wet methods, including sol–gel and electrochemical deposition, have the advantages of low production costs and high flexibility, which makes them a promising alternative to dry application methods [82].

Sol-gel is mainly used to coat HA on various implants, which involves two successive stages, including (1) the preparation of sol, which is a colloidal suspension containing a dissolved precursor in a solvent, and (2) the manufacture of gel by polycondensation prepared salt. Usually, the sol–gel method can be carried out in an aqueous or alcoholic medium. In addition, the precursors used in this method are alkoxide or non-alkoxide. The precursor of alkoxides is more volatile. To prepare the sol used for the application of HA coatings, Ca and P must be added to the appropriate solvent consisting of ethanol and a small amount of water. The purpose of adding water is to accelerate the hydrolysis of sol. Usually, calcium and phosphorus precursors in the preparation of sol are calcium nitrate ($Ca(NO_3)_2$) and phosphorus pentoxide (P_4O_{10}) or triethyl phosphite ($P(OEt)_3$; $C_6H_{15}O_3P$), respectively [83, 95].

The prepared sol can be applied to the substrate either by immersion coating or by centrifugation, while the immersion coating includes three stages: immersion, removal, and drying. The coating by centrifugation refers to a method, in which sol is applied to the centre of the spinning substrate until it spreads and completely covers the substrate [96, 97]. Figure 3 schematically shows the process of coating by centrifugation for HA coating manufacture.

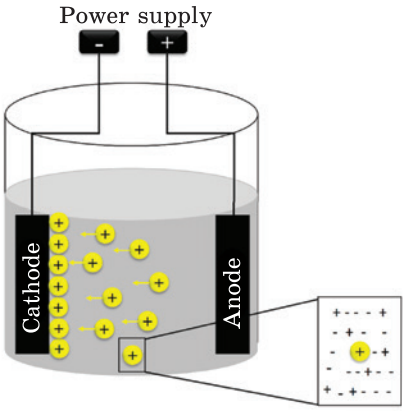

Fig. 4. Schematic representation of a standard installation for electrophoretic deposition (EPD) of HA coatings [91]

The advantage of this method is the possibility of obtaining a stoichiometric ratio Ca/P = 1.67, which is much more difficult to obtain by other methods. This method is of the greatest interest due to the low heat treatment of the surface (350 °C). Classical methods were carried out during heat treatment in the region of 600–800 °C and more. Such a low crystallization temperature of HA prevents any changes in the structure of the metal substrate. Coatings obtained from solutions form a continuous gas-tight film on the metal surface and have a number of valuable qualities: a lower melting point than slip coatings, a small thickness, and, consequently, greater flexibility. At the same time, such advantages as the simplicity of hardware design, the possibility of synthesizing fundamentally new compositions, and the high purity of the materials obtained explain the significant interest shown in the technology.

Electrochemical deposition can be divided into chemical deposition, electrophoretic deposition (EPD) and, the main topic of this master's thesis, electrodeposition (ED). Electrodeposition has become more interesting for the development of highly efficient HA. Non-metallic substrates, such as polymer mesh or porous ceramics, can be metalized by chemical deposition after appropriate preliminary sensitization and activation [98].

EPD is often performed in a two-electrode cell at a constant cell voltage. That is a well-known colloidal technology for ceramic coatings manufacture, in which charged suspended/dispersed particles move through a liquid medium and are deposited on a conductive substrate. Usually, the size of suspended particles should not exceed 30 microns [99].

EPD allows applying both pure HA and HA-based composite coatings to metal implants. Commonly used chemicals for HA electrolyte preparation in the EPD process include HA particles, solvents, and dispersants. Usually, *n*-butanol and triethanolamine serve as a solvent and dispersants, respectively [100]. The standard EPD scheme of HA coatings is shown in Fig. 4.

It should be noted that Fig. 4 shows a diagram of the cathode EPD, since positively charged particles move to the cathode, that is, to a negatively charged electrode. The EPD of negatively charged particles is known as the anodic EPD [101].

Electrodeposition, a widely used coating method, refers to a process in which the anode material is dissolved by an electric current followed by displacement. It is worth noting that anodes can be sacrificial or inert. At the cathode/electrolyte interface, the number of ions is restored, and a coating of the desired composition is applied to the cathode surface. Electrodeposition can also be carried out by anodic oxidation of dissolved particles. The electrolyte provides an electrical circuit between the electrodes in the cell. Electrodeposition opens up promising opportunities for HA coatings manufacture as an alternative to dry methods, especially, plasma spraying. During the electrodeposition of HA, calcium-containing and phosphorus-containing salts are dissolved in water to prepare the electrolyte. This method takes advantage of the pH-dependent solubility of calcium phosphate salts. Recently, many attempts have been made to optimize the operating parameters. The following section, in detail, discusses the mechanisms that control the coating during the electrodeposition process.

On the other hand, the EPD process is a sufficiently fast and inexpensive method that demonstrates some advantages over alternative processes. Some of these advantages are the simplicity of the method, the ability to form complex shapes and patterns, control of the thickness and morphology of the coating, and the low-temperature ability to manufacture products [102] for medical purposes. Moreover, it is now well established that the particle size and the degree of agglomeration of ceramic powders are essential factors for the quality of the coating. Structures that do not contain agglomerates, made of densely packed small particles, can be compacted at lower sintering temperatures.

In Ref. [103], using $Ca(NO_3)_{24}H_2O$, $(NH_4)_2HPO_4$ and NH_4OH as starting materials, samples were synthesized by precipitation during cold drying for 72 h and subsequent annealing at 800 °C for 1 h. As a result, HA samples turn out to be stoichiometric (after annealing Ca/P = 1.66), and according to morphological studies they have a micron size of crystallites (0.55–1.2 μm in diameter and 2.3–2.9 μm in length). These samples find practical application in medicine when filling bone defects (in case of loss of a part of the bone, to accelerate the tissue regeneration processes) or in dental pastes. Processes involving low-temperature treatment of the precipitate in semi-continuous synthesis using solutions of (3.06 M) calcium chloride ($CaCl_2$) and (0.38 M) (K_2HPO_4) provide materials studied on XRF (Rigaku Rotaflex RU-200B), HVEM (JEOL 1210 at 120 kV) and IR (Nicolet 710) having according to the analysis of XRF and HVEM 60–90 nm and from 60–200 nm, respectively. IR spectroscopy data reveal all modes of oscillations characterizing hydroxyapatite. The measurements have shown that with the predominance of HPO_4 ions over Ca ions in the initial solutions, a HA is formed with a stoichiometric ratio Ca/P = 1.67, in the opposite case, a violation of stoichiometry Ca/P = 1.53 is manifested.

The method of microarc oxidation (MAO) in aqueous solutions of electrolytes is considered the most convenient and effective method for calcium phosphate coatings formation with quality physicochemical properties on products of complex shape, also referred to as implants. This method is also known as microplasma or plasma-electrolytic oxidation.

The MAO process has been studied most fully for valve metals and their alloys (aluminium, magnesium, titanium, tantalum, niobium, zirconium, *etc.*). The PEO process makes it possible to obtain multifunctional coatings with a unique set of properties, including wear-resistant, corrosion-resistant, heat-resistant, electrical insulation, and decorative. Therefore, the scope of application of these coatings is quite wide: medicine, aviation, ship, instrument, automotive and other industries.

In the invention of the Shanghai Institute of Ceramics (China) [104], MAO using ultrasound is used to obtain coatings on a titanium implant. This method produces a porous antibacterial coating containing elements Ca, P, and Ag, which increase biological activity and corrosion resistance. Characteristics of the resulting coating: thickness of 50–85 microns, pore diameter of 4–25 microns, porosity of 20–30%, adhesion strength to the substrate of 23–40 MPa.

According to the technology developed by the Dalian University of Technology (China), a nanoporous film of titanium dioxide is obtained as a biomaterial as a result of MAO in a solution containing sodium tetraborate [105]. Using this electrolyte and a certain process mode makes it possible to obtain a coating with excellent wettability and resistance to destruction. It is established that the resulting titanium dioxide is rutile.

Coatings obtained by this method have high physical and mechanical characteristics, but a low ratio of Ca and P (Ca/P = 0.13) compared to that for bone tissue (Ca/P = 1.67), although, there are known works, in which a ratio of Ca/P = 0.45 or more was obtained [106]. Tests of GA-coated samples obtained by the MAO method for fatigue strength do not reveal a significant decrease in the fatigue characteristics of the coating compared to the substrate material. Due to the relative simplicity of the coating process, MAO is one of the main methods for HA coatings. Due to the high temperature that occurs in microplasma discharges, coatings in the melted state are formed on the metal surface in the electrolyte, which ensures strong adhesion to the substrate.

The disadvantage of this method is the low Ca/P ratio in the coating, but it is possible to obtain films with a thickness of about 80 microns. By the MAO method, it is impossible to apply a HA coating on stainless steel (as a result of the formation of Fe oxide, which dissolves quickly). When obtaining HA coatings by this method on titanium, free titanium appears in them along with HA, which can negatively affect the biological properties of implants [107].

Magnetron sputtering systems are technological devices that allow forming thin film coatings by cathodic sputtering of the target material in magnetron discharge plasma. The principle of operation of this type of device is based on the formation of electric and magnetic fields directed perpendicular to each other in the cathode region.

The magnetic field, whose lines of force are parallel to the surface of the sputtered magnetron target, holds electrons near the target in the so-called electronic 'trap' created by crossed electric and magnetic fields. The movement of electrons along spiral trajectories ensures high plasma density at low working gas pressure and a high sputtering rate of the target material.

When a negative voltage is applied to the cathode, a glow discharge is excited. Electrons emitted from the cathode under the action of bombardment by ions of the working gas are captured by a magnetic field. There is an electron trap created, on the one hand, by a magnetic field that returns electrons to the cathode, and on the other hand, by a target under a negative potential that repels electrons that oscillate in this trap until several ionizing collisions with atoms of the working gas occur.

The magnetic field ensures the localization of plasma at the target surface. The cathode surface is sprayed in the area located above the poles of the magnetic system. As a result, an erosion zone is formed in the form of a closed track, the geometry of which is determined by a magnetic system (Fig. 5) [108].

5. Coatings Formation

When developing new types of composite materials, which are a coating on the surface of a bioinert alloy, it is essential to be able to control the structure, and, consequently, the service properties of the biocomposite. There are known works of various scientific groups dealing with the formation of coatings obtained by RF magnetron sputtering of targets based on various calcium phosphates, such as HA [71, 109], tricalcium phosphate (TCP) [110, 111], tetracalcium phosphate [110], as well as calcium pyrophosphate [112, 113] and calcium metaphosphate [114]. However, up to 80% of the work is devoted to the use of HA-based targets.

It should be noted that the elemental composition and morphology of both biological and synthetic calcium hydroxyapatite differs depending on the formation and production conditions: the pH of the medium, and the presence of third-party atoms and groups in the matrix solution. It is amusing that defects in the form of two-dimensional (2*D*) and three-dimensional (3*D*) formations with a rod-shaped, spherical, fractal, and even lamellar (like 2*D* fragments [115–117]) structures were observed depending on the method of obtaining HA and for biogenic HA, *i.e.*, on the age and area of bone tissue. It is clear that when admixture

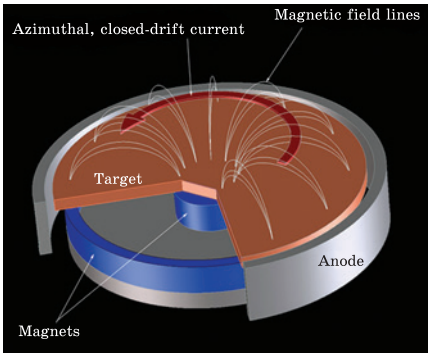

◀ *Fig. 5*. Magnetron sputtering system with flat target [108]

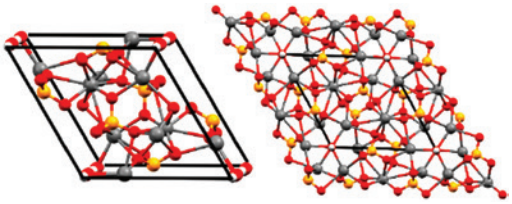

Fig. 6. HA crystal structure (left) and HA projection structure in the (001) plane (right) [125]

atoms and a large percentage of isomorphic substitutions are included in the hydroxyapatite composition, the crystal lattice will undergo distortions with a possible change in the size of the unit cell and its volume, which is recorded by RD and electron microscopy methods. When considering the parameters of the unit cell of the HA, it becomes obvious that, depending on the radius of the substituent ion, as well as on its percentage content in the HA, both simultaneous changes in parameters a and c and change in one of the two depending on the substitution position are possible.

It is experimentally known that the most likely change is parameter a, whereas parameter c changes weakly.

As a rule, the main criteria for determining the possibility of using a particular biocoating is the morphology of the coating surface, its structure, phase composition, and crystallinity, since these parameters are responsible for one of the essential indicators, namely, the intensity of bioresorption of the coating. In this paper, the possibility of controlling the structure of high-frequency magnetron coatings using: a) changes in the parameters of the spraying process (supply of positive/negative displacement to the substrate and the use of reaction gas); b) changes in the substrate temperature (in the range from 100 to 400 °C); c) changes in the plasma composition (using targets with different contents of hydroxyapatite and tricalcium phosphate phases) [118–123].

Living organisms can crystallize and deposit various minerals during biomineralization processes, for example, such as CaP [124]. Attempts to determine the chemical structure and composition of CaP, formerly called apatites, began in the middle of the 18th century. However, it was only in the XIX century that the existence of different phases of CaP was suggested [124].

The most common HA structure belongs to the hexagonal system with the space group $P63/m$, demonstrating symmetry perpendicular to the three equivalent axes a (a_1, a_2, and a_3), which form angles of 120° to

each other. Its unit cell consists of calcium (Ca) and phosphates and can be represented by $M_{14}M_{26}(PO_4)_6(OH)_2$, in which M_1 and M_2 represent two different crystallographic positions for 10 calcium atoms. Four Ca atoms are surrounded by nine oxygen (O) in the PO_4 tetrahedron. The other six Ca atoms are surrounded by the remaining six O atoms and one of the two OH [125].

Figure 6 schematically shows the gradient coverage of the HA obtained by applying dynamic voltage. The layer directly adjacent to the titanium substrate consisted of small particles, where there were very few opportunities for the deposition of large particles due to low voltage. When the voltage was increased, the coatings consisted of larger particles. It has also been proposed that a uniform, tightly packed layer of nanoscale particles reach 64% of the theoretical density. However, it was likely that the layer containing particles of various sizes had a density of up to 73. That happened because the smaller particles filled the gaps between the larger particles. In light of the results of this study, dynamic stress EPD has reasonably established itself as a promising method for obtaining dense coatings.

Sintering of electrophoretic deposition (EPD) coatings resulted in coatings showing well-defined HA peaks. In other words, the phase structure of the resulting coating from the HA was not disturbed during sintering.

HA is of great interest in the sphere of biomedicine for various applications, such as implants or prostheses in orthopaedics, maxillofacial, and dentistry, intending to restore or replace hard tissues. That is due to its excellent biocompatibility and biological activity, resulting from its chemical analogy with mineral compounds of human bones and the hard tissues of teeth, as mentioned earlier [124]. In addition, the HA has good mechanical strength, porous structure, and osteoconductive, osteoinductive, and osseointegrated properties [125]. HA can be used as an implant material in the form of a solid with low porosity, granular particles, porous structures, and loads. In addition, it can be used as a coating on metal implants, improving their biocompatibility [58]. When an HA-based material is implanted, a free layer of fibrous tissue consisting of carbonized apatite forms on its surface, which promotes the attachment of the implant to living bone, that is, improves the fixation of the implant in the surrounding tissues [125]. HA can promote the growth of new tissue through the osteoconduction mechanism without causing systemic or local toxicity, inflammation, or similar reactions caused by other foreign bodies. The porosity of the GAP is one of the most important factors for controlling the characteristics of the implant since the structure with open pores ensures the diffusion of cells responsible for the deposition of bone tissue, which provides better biointegration and mechanical stability of the implant. HA can also be

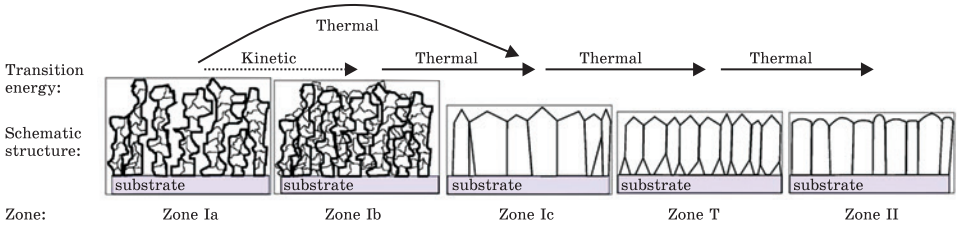

Fig. 7. Schematic representation of the extended structural zone model (ESZM) proposed by S. Mahieu *et al.* [126]

used as solid scaffolds for tissue repair in tissue engineering to model compounds for biomineralization of the human body, inhibition of the growth of many types of cancer cells, drug supply, restoration of tooth enamel, and injectable bone cement. The mixture of HA with other phosphates, such as tricalcium phosphate (TCP), provides greater applicability of this material since it provides greater cell adhesion and osteogenic characteristics [125]. However, using porous material is limited to areas where the skeleton is not required mechanically or as a filling of bone cavities since it has low mechanical resistance.

The author of Ref. [126], based on the study of the structure of TiN coatings formed by reactive magnetron sputtering, proposed an extended structural zone model (ESZM), in which, in addition to the homological temperature of the substrate and the kinetic energy of adatoms, the processes of diffusion, nucleation, and recrystallization, depending on the mobility of adatoms, are taken into account. The characteristic features of the corresponding zones in the ESZM are shown in Fig. 7 [126]. According to ESZM, with an increase in the energy flow supplied to the growth surface, the mobility of adatoms increases, which determines the formation of a characteristic microstructure of a thin film.

Zones *Ia* and *Ib* describe the structure of coatings formed under conditions of low energy supply to the substrate from the plasma side. At the same time, the mobility of adatoms is practically absent. Under such conditions, an amorphous film is formed. Zone *Ia* is characterized by a porous structure; with an increase in the bombardment of the coating by flying particles, it becomes denser and is determined by zone *Ib*. A further increase in the thermal power of the plasma or the energy supplied to the condensation surface leads to a transformation of the structure with the formation of a textured film, the grains of which are differently oriented relative to each other (zone *Ic*).

In conditions, when the mobility of adatoms is sufficient for their intergranular diffusion, the *T* area is formed. In this case, the mechanism of the evolutionary growth of the coating grains in the direction with the highest growth rate is manifested. The microstructure is characterized by *V*-shaped crystal blocks oriented perpendicular to the sub-

strate. A further increase in the energy flow leads to an increase in the coating textured with planes with the lowest surface energy. Under these conditions, the film structure is determined by the processes of recrystallization and migration of grain boundaries (zone *II*).

The author of the work [127] showed that zone structural models of coating formation are equally valid for ion-plasma films and coatings, as well as for vacuum-arc or gas-phase ones. In addition, the results of the studies obtained within the framework of the presented work indicate the commonality of the formation patterns of the microstructure of coatings formed by magnetron sputtering of targets from various materials.

6. Conclusions

Coatings based on synthetic and biological hydroxyapatite on the surface of ultrafine-grained titanium and zirconium have been developed and improved in the world for many years, so this review is very relevant. Based on this, the article presents the issues of obtaining such coatings and analyses the possibilities of practical improvement of the physical and mechanical properties of bioinert alloys due to the formation of an ultrafine-grained/nanostructured state by methods of intensive plastic deformation. The results of studies of the microstructure and mechanical properties of titanium and zirconium in nanostructured and ultrafine-grained states obtained by methods of intensive plastic deformation are presented. Solutions to the problems of coating formation on the surface of coarse-grained and ultrafine-grained bioinert titanium and zirconium alloys are proposed. Convincingly shown that coatings applied to the surface of titanium and zirconium alloys in a coarse-grained and ultrafine-grained state increase their corrosion resistance in physiological solutions and aggressive environments, that is due to a combination of high values of the electrical resistance of the nonporous oxide sublayer of coatings, the activation energy of the corrosion process, as well as their adhesive strength.

REFERENCES

1. E. Chicardi, C.F. Gutiérrez-González, M.J. Sayagués, and C. García-Garrido, *Materials and Design*, **145**: 88–96 (2018); https://doi.org/10.1016/j.matdes.2018.02.042
2. K.M. Reyes, N.K. Kuromoto, A.P.R. Alves Claro, and C.E.B. Marino, *Mater. Res. Express*, **4**: 075402 (2017); https://doi.org/10.1088/2053-1591/aa6ee4
3. I.E. Volokitina, *Metal Science and Heat Treatment*, **63**, Nos. 3–4: 163 (2021); https://doi.org/10.1007/s11041-021-00664-y
4. I.E. Volokitina, *Journal of Chemical Technology and Metallurgy*, **55**: 479 (2020).
5. S. Lezhnev, A. Naizabekov, and E. Panin, *Procedia Engineering*, **81**: 1499 (2014); https://doi.org/10.1016/j.proeng.2014.10.180

6. B. Sapargaliyeva, A. Agabekova, G. Ulyeva, A. Yerzhanov, and P. Kozlov, *Case Studies in Construction Materials*, **18**: e02162 (2023); https://doi.org/10.1016/j.cscm.2023.e02162
7. S. Syrlybekkyzy, R. Fediuk, A. Yerzhanov, R. Nadirov, A. Utelbayeva, A. Agabekova, M. Latypova, L. Chepelyan, N. Vatin, A. Kolesnikov, and M. Amran, *Materials*, **15**: 6980 (2022); https://doi.org/10.3390/ma15196980
8. M.A. Latypova, V.V. Chigirinsky, and A.S. Kolesnikov, *Progress in Physics of Metals*, **24**: 132–156 (2023); https://doi.org/10.15407/ufm.24.01.132
9. A. Naizabekov, S. Lezhnev, E. Panin, A. Arbuz, T. Koinov, and I. Mazur, *Materials Engineering and Performance*, **28**: 200–210 (2019); https://doi.org/10.1007/s11665-018-3790-z
10. C.E. Lekka, J.J. Gutiérrez-Moreno, and M. Calin, *Journal of Physics and Chemistry of Solids*, **102**: 49–61 (2017); https://doi.org/10.1016/j.jpcs.2016.10.013
11. I.V. Okulov, A.S. Volegov, H. Attar, M. Bönisch, S. Ehtemam-Haghighi, M. Calin, and J. Eckert, *Journal of the Mechanical Behavior of Biomedical Materials*, **65**: 866–871 (2017); https://doi.org/10.1016/j.jmbbm.2016.10.013
12. S. Lezhnev and A. Naizabekov, *Journal of Chemical Technology and Metallurgy*, **52**: 626–635 (2017).
13. S. Lezhnev, A. Naizabekov, and A. Volokitin, *Procedia Engineering*, **81**: 1505–1510 (2014); https://doi.org/10.1016/j.proeng.2014.10.181
14. A. Bychkov and A. Kolesnikov, *Metallography, Microstructure, and Analysis*, **12**, No. 3: 564–566 (2023); https://doi.org/10.1007/s13632-023-00966-y
15. I.E. Volokitina and A.V. Volokitin, *Metallurgist*, **67**: 232–239 (2023); https://doi.org/10.1007/s11015-023-01510-7
16. A. Kolesnikov and O. Kolesnikova, *Metallurgist*, **66**, Nos. 11–12: 1601–1606 (2023).
17. A. Volokitin, A. Naizabekov, and I. Volokitina, *Journal of Chemical Technology and Metallurgy*, **57**: 809 (2022).
18. I.E. Volokitina, A.V. Volokitin, and E.A. Panin, *Metallography, Microstructure, and Analysis*, **11**: 673–675 (2023); https://doi.org/10.1007/s13632-022-00877-4
19. A. Naizabekov, A. Arbuz, S. Lezhnev, and E. Panin, *Physica Scripta*, **94**, No. 10: 105702 (2019); https://doi.org/ 10.1088/1402-4896/ab1e6e
20. W. Lacefield, *An Introduction in Bioceramics* (New York: 1996).
21. Y. Ikarashi, T. Tsuchiya, and A. Nakamura, *Proc. Fifth World Biomaterials Congress* (Toronto: Canada: 1996).
22. S.G. Steinemann and S.M. Persen, *Ti'84 Science and Technology* (DGM: 1984).
23. R. Thull, *Z. Mitteilungen*, **82**: 39–45 (1992).
24. R. Thull, *Medical Progress Through Technology*, **5**: 103–112 (1977).
25. B. Kasemo and J. Lausmaa, *Osseointegration in Clinical Dentistry*: 99–115 (1985).
26. E. Merian, *Metalle in der Umwelt. Verteilung, Analytik und biologische Relevanz.* (Weinheim: Verlag Chemie: 1984), p. 12–17
27. G.K. Smith, *Systematic Aspects of Biocompatibility*, II: 1–22 (1981).
28. K. Gomi, S. Saiton, M. Kanazashi, T. Arai, and J. Nakamura, *Proc. Fifth World Biomaterial Congress* (1996), p. 741.

29. N. Vasilyeva, R. Fediuk, and A. Kolesnikov, *Materials*, **15**: 3975 (2022); https://doi.org/10.3390/ma15113975
30. A.B. Nayzabekov and I.E. Volokitina, *Physics of Metals and Metallography*, **120**, No. 2: 177–183 (2019); https://doi.org/10.1134/S0031918X19020133
31. E. Palazzo, *International Journal of Legal Medicine*, **125**: 21–26 (2009); https://doi.org/10.1007/s00414-009-0394-z
32. S.M. Jafari, *Clinical Orthopaedics and Related Research*, **468**: 2046–2051 (2010); https://doi.org/10.1007/s11999-010-1251-6
33. S. Mandl and B. Rauenbach, *Surface and Coatings Technology*, **156**: 583–589 (2002); https://doi.org/10.1016/S0257-8972(02)00085-3
34. R.Z. Valiev, A.V. Sergueeva, and A.K. Mukherjee, *Scripta Mater.*, **49**: 666–674 (2003); https://doi.org/10.1016/S1359-6462(03)00395-6
35. M. Hawryluk, J. Ziemba, and P. Sadowski, *Materials Science*, **50**: 74–78 (2017); https://doi.org/10.1177/0020294017707161
36. A.B. Naizabekov and S.N. Lezhnev, *Metal Science and Heat Treatment*, **57**, No. 5–6: 254–260 (2015); https://doi.org/ 10.1007/s11041-015-9870-x
37. S. Lezhnev and E. Panin, *Advanced Materials Research*, 814: 68–75 (2013); https://doi.org/10.4028/www.scientific.net/AMR.**814**.68
38. I.E. Volokitina, *Metal Science and Heat Treatment*, **61**: 234 (2019); https://doi.org/10.1007/s11041-019-00406-1
39. G. Raab, A. Raab, R. Asfandiyarov, and E. Fakhretdinova, *Non-Eequilibrium Phase Transformations*, 1: 10–11 (2017).
40. S. Dobatkin, J. Zrnik, and I. Mamuzi, *Metalurgija*, **49**: 343–347 (2010).
41. I.E. Volokitina, *Metal Science and Heat Treatment*, **62**: 253 (2020); https://doi.org/10.1007/s11041-020-00544-x
42. I. Volokitina and A. Volokitin, *Physics of Metals and Metallography*, **119**, No. 9: 917–921 (2018); https://doi.org/ 10.1134/S0031918X18090132
43. A. Naizabekov and E. Panin, *Journal of Materials Engineering and Performance*, 28, No. 3: 1762 (2019).
44. R.Z. Valiev, *Investigations and Applications of Severe Plastic Deformation* (Netherlands: Springer: 2000), p. 221–230.
45. E. Mostaed, A. Fabrizi, F. Bonollo, and M. Vedani, *Metallurgia Italiana*, **107**, No. 11: 5–12 (2016).
46. N. Zhangabay, B. Sapargaliyeva, U. Suleimenov, K. Abshenov, A. Utelbayeva, K. Baibolov, R. Fediuk, D. Arinova, B. Duissenbekov, A. Seitkhanov, and M. Amran, *Materials*, **15**: 5732 (2022); https://doi.org/10.3390/ma15165732
47. C. Banjongprasert, A. Jak-Ra, C. Domrong, U. Patakham, W. Pongsaksawad, and T. Chairuangsri, *Archives of Metallurgy and Materials*, **60**: 887–890 (2015); https://doi.org/10.1515/amm-2015-0224
48. M.I. Latypov, M.G. Lee, Y. Beygelzimer, D. Prilepo, Y. Gusar, and H.S. Kim, *Metallurgical and Materials Transactions A*, **47**: 1248–1260 (2016); https://doi.org/10.1007/s11661-015-3298-1
49. I.E. Volokitina, *Journal of Chemical Technology and Metallurgy*, **57**: 631–636 (2022).
50. A. Volokitin and D. Kuis, *Journal of Chemical Technology and Metallurgy*, **56**, No. 3: 643–647 (2021).

51. I.E. Volokitina, A.V. Volokitin, and E.A. Panin, *Progress in Physics of Metals*, **23**, No. 4: 684–728 (2022);
https://doi.org/10.15407/ufm.23.04.684
52. G.A. Salishchev, R.M. Galeyev, O.R. Valiakhmetov, R.V. Safiulin, R.Y. Lutfullin, O.N. Senkov, F.H. Froes, and O.A. Kaibyshev, *Journal of Materials Processing Technology*, **116**: 265–268 (2001);
https://doi.org/10.1016/S0924-0136(01)01037-8
53. S.V. Zherebtsov, G.A. Salishchev, R.M. Galeyev, O.R. Valiakhmetov, S.Y. Mironov, and S.L. Semiatin, *Scripta Mater.*, **51**: 1147–1151 (2004);
https://doi.org/ 10.1016/j.scriptamat.2004.08.018
54. B.B. Straumal, A.A. Mazilkin, S.G. Protasova, D. Goll, B. Baretzky, A.S. Bakai, and S.V. Dobatkin, *Kovove Mater.*, **49**: 17–22 (2011);
https://doi.org/10.4149/km-2011-1-17
55. Y.G. Ko, W.S. Jung, D.H. Shin, and C.S. Lee, *Scripta Mater.*, **48**: 197–202 (2003);
https://doi.org/10.1016/s1359-6462(02)00356-1
56. S.M. Kim, J. Kim, D.H. Shin, Y.G. Ko, C.S. Lee, and S.L. Semiatin, *Scripta Mater.*, **50**: 927–930 (2004);
https://doi.org/10.1016/j.scriptamat.2004.01.020
57. S.L. Semiatin and T.R. Bieler, *Acta Mater.*, **49**: 3565–3573 (2001).
58. A. Ambard, L. Guetaz, F. Louchet, and D. Guichard, *Mater. Sci. Eng. A*, **319–321**: 404–408 (2001);
https://doi.org/10.1016/S0921-5093(00)02003-7
59. G.H. Atmaram, H. Mohammed, and F.J. Schoen, *Biomater. Med. Devices Artif. Organ*, **7**: 99–104 (1979);
https://doi.org/10.3109/10731197909119376
60. Y. Sharkeev, A. Eroshenko, E. Legostaeva, Z. Kovalevskaya, O. Belyavskaya, M. Khimich, M. Epple, O. Prymak, V. Sokolova, Q. Zhu, S. Zeming, and Z. Hongju, *Metals*, **12**, No. 7: 1136 (2022);
https://doi.org/10.3390/met12071136
61. N.V. Bekrenev, V.N. Liasnikov, and D.V. Trofimov, *Method of Plasma Spraying of Coatings. Patent RF No. 2283364* (Published 10.09.2006).
62. P. Prevey, *J. Thermal Spray Tech.*, **9**: 369–376 (2000).
63. K.D. Roger and S.E. Etok, *J. Mater. Sci.*, **39**: 5747–5754 (2004);
https://doi.org/10.1023/B:JMSC.0000040085.43633.8a
64. L.A. De Sena, M.C. Andrade, A.M. Rossi, and G.D. Soares, *J. Biomed. Mater. Res.*, **60**: 1–7 (2002);
https://doi.org/ 10.1002/jbm.10003
65. E.P. Aves and G.F. Estevez, *J. Mater. Sci.*, **20**: 543–547 (2009);
https://doi.org/10.1007/s10856-008-3609-9
66. H-W. Kim, H-E. Kim, and J.C. Knowles, *J. Amer. Ceram. Soc.*, **88**: 154–159 (2005).
67. T. Kokubo and H. Takadama, *Biomaterials*, **27**: 2907–2915 (2006);
https://doi.org/ 10.1016/j.biomaterials.2006.01.017
68. X. Chen, A. Nouri, and Y. Li, *Biotechnol. Bioeng.*, **101**: 378–387 (2008);
https://doi.org/10.1002/bit.21900
69. A.R. Boyd, B.J. Meenan, and N.S. Leyland, *Surface and Coating Technology*, **200**, Nos. 20–21: 6002–6013 (2006);
https://doi.org/10.1016/j.surfcoat.2005.09.032
70. V.F. Pichugin, M.A. Surmeneva, R.A. Surmenev, I.A. Khlusov, and M. Epple, *Journal of Surface Investigation. X-Ray, Synchrotron and Neutron Techniques*,

5, No. 5: 863–869 (2011);
https://doi.org/10.1134/S1027451011090138
71. R.A. Surmenev, *Surf. Coat. Technol.*, **206**, Nos. 8–9: 2035–2056 (2012);
https://doi.org/10.1016/j.surfcoat.2011.11.002
72. Y.N. Tyurin and A.P. Arbuzov, *Method of Applying Detonation Coating. USSR Author's Cert. No. 1045491* (1983).
73. V.A. Popov and E.A. Mironov, *Installation for the Detonation Spraying of Powder Materials. Inventor's Note. USSR Author's Cert. No. 551053.*
74. V.V. Stolyarov, *Journal of Ultrafine Grained and Nanostructured Materials*, **55**, No. 1: 10–14 (2022);
https://doi.org/10.22059/jufgnsm.2022.01.02
75. M. Asgari, M. Honarpisheh, and H. Mansouri, *Journal of Ultrafine Grained and Nanostructured Materials*, **53**, No. 1: 48–59 (2020);
https://doi.org/10.22059/jufgnsm.2020.01.07
76. W.B. Donohue and C. Maseres, *Oral Maxillofac Surgery*, **48**: 1196–1200 (1990).
77. L. Tuantuan and H. Aoki, *12th Eur. Conf. on Biomaterials* (1995), p. 63.
78. C.M. Horwitz, *J. Vac. Sci. Technol. Bd.*, **1**: 60–68 (1983).
79. W.S. Harun, R.I. Asri, J. Alias, F.H. Zulkifli, K. Kadirgama, S.A. Ghani, and J.H. Shariffuddin, *Ceramics International*, **44**: 1250–1268 (2018);
https://doi.org/10.1016/j.ceramint.2017.10.162
80. S. Vahabzadeh, M. Roy, and A. Bandyopadhyay, *Acta Biomaterialia*, **17**: 47–55 (2015);
https://doi.org/10.1016/j.actbio.2015.01.022
81. H. Melero, M. Torrell, J. Fernández, J.R. Gomes, and J.M. Guilemany, *Wear*, **305**: 8–13 (2013);
https://doi.org/10.1016/j.wear.2013.05.009
82. B. Fotovvati, N. Namdari, and A. Dehghanghadikolaei, *Journal of Manufacturing and Materials Processing*, **3**, No. 1: 28–32 (2019);
https://doi.org/10.3390/jmmp3010028
83. G. Choi, A.H. Choi, L.A. Evans, S. Akyol, and B. Ben-Nissan, *Journal of the American Ceramic Society*, **103**, No. 10: 5442–5453 (2020);
https://doi.org/10.1111/jace.17118
84. A.V. Rane, K. Kanny, V.K. Abitha, and S. Thomas, Methods for Synthesis of Nanoparticles and Fabrication of Nanocomposites, *Synthesis of inorganic nanomaterials* (Woodhead Publishing: 2018), Ch. 4, p. 121–139;
https://doi.org/10.1016/B978-0-08-101975-7.00005-1
85. D. Milovac, *Materials Science and Engineering C*, **34**: 437–445 (2014);
https://doi.org/10.1016/j.msec.2013.09.036
86. A. Pal, S. Maity, S. Chabri, S. Bera, A.R. Chowdhury, M. Das, and A. Sinha, *Biomedical Physics & Engineering Express*, **3**: 015010 (2017);
https://doi.org/10.1088/2057-1976/aa54f5
87. S.K. Padmanabhan, *Journal of Nanoscience and Nanotechnology*, **15**, No. 1, 504–509 (2015);
https://doi.org/10.1166/jnn.2015.9489
88. F. Heidari, M.E. Bahrololoom, D. Vashaee, and L. Tayebi, *Ceramics International*, **41**: 3094–3100 (2015);
https://doi.org/10.1016/j.ceramint.2014.10.153
89. F. Chen, W.M. Lam, C.J. Lin, G.X. Qiu, Z.H. Wu, K.D. Luk, and W.W. Lu, *Journal of Biomedical Materials Research Part B: Applied Biomaterials*, **82B**, No. 1: 183–191 (2007);
https://doi.org/10.1002/jbm.b.30720

90. C. Pierlot, L. Pawlowski, M. Bigan, and P. Chagnon, *Surface and Coatings technology*, **202**: 4483–4490 (2008); https://doi.org/10.1016/j.surfcoat.2008.04.031
91. M.S. Safavi, F.C. Walsh, M.A. Surmeneva, R.A. Surmenev, and J. Khalil-Allafi, *Coatings*, **11**, No. 1: 110–118 (2021); https://doi.org/10.3390/coatings11010110
92. W.S. Harun, R.I. Asri, J. Alias, F.H. Zulkifli, K. Kadirgama, S.A. Ghani, and J.H. Shariffuddin, *Ceramics International*, **44**: 1250–1268 (2018); https://doi.org/10.1016/j.ceramint.2017.10.162
93. A.S. Kolesnikov, *Russ. J. Non-Ferrous Metals,* **55**: 513–518 (2014); https://doi.org/10.3103/S1067821214060121
94. A.K. Lynn and D.L. DuQuesnay, *Biomaterials*, **23**: 1937–1946 (2002); https://doi.org/10.1016/S0142-9612(01)00321-0
95. S.F. Robertson, A. Bandyopadhyay, and S. Bose, *Surface and Coatings Technology*, **372**: 140–147 (2019); https://doi.org/10.1016/j.surfcoat.2019.04.071
96. S. Kumar, S. Saralch, U. Jabeen, and D. Pathak, *Colloidal Metal Oxide Nanoparticles. Synthesis, Characterization and Applications*, (Elsevier: 2020), p. 471–504; https://doi.org/10.1016/B978-0-12-813357-6.00017-6
97. A.Ç. Kılınç, S. Köktaş, and A.A. Göktaş, *Journal of the Australian Ceramic Society*, **57**: 47–53 (2021); https://doi.org/10.1007/s41779-020-00511-y
98. F.C. Walsh and C. Larson, *Transactions of the IMF*, **98**, No. 6: 288–299 (2020); https://doi.org/10.1080/00202967.2020.1819022
99. Y. Ma, J. Han, M. Wang, X. Chen, and S. Jia, *Journal of Materiomics*, **4**: 108–120 (2018); https://doi.org/10.1016/j.jmat.2018.02.004
100. N. Horandghadim, J. Khalil-Allafi, and M. Urgen, *Surface and Coatings Technology*, **386**: 125458 (2020); https://doi.org/10.1016/j.surfcoat.2020.125458
101. L. Besra and M. Liu, *Progress in Materials Science*, **52**: 1–61 (2007); https://doi.org/10.1016/j.pmatsci.2006.07.001
102. Y.F. Chou, W.A. Chiou, Y. Xu, J.C. Dunn, and B.M. Wu, *Biomaterials*, **25**: 5323–5331 (2004); https://doi.org/10.1016/j.biomaterials.2003.12.037
103. J. Gymez-Morales, J. Torrent-Burgués, T. Boix, J. Fraile, and R. Rodríguez-Clemente, *Cryst. Res. Technol.*, **36**: 15–26 (2001); https://doi.org/10.1002/1521-4079(200101)36:1<15::AID-CRAT15>3.0.CO;2-E
104. *Preparation Method of Ultrasonic Microarc Oxidation Silver-Carrying Antibiotic Bioactive Coating on Magnesium and Titanium Surface. Patent No. 101899700, CN* (Publ. 01.12.2010).
105. *Preparation Process of Pleated Hole-Slot Shaped Titanium Dioxide Thin Film with Super Wetting Ability. Patent No. 102605411, CN* (Publ. 25.07.2012).
106. P. Wang, L. Zhao, J. Liu, M.D. Weir, X. Zhou, and H.H.K. Xu, *Bone Research.*, **2**: 14017 (2014); https://doi.org/0.1038/boneres.2014.17
107. D.M. Liu, H.M. Chou, and O.V. Wu, *J. Mater. Sci. Mater. Mad.*, **5**: 147–153 (1994); https://doi.org/10.1007/BF00053335
108. A. Anders, *Surface and Coatings Technology*, **205**: S1–S9 (2011); https://doi.org/10.1016/j.surfcoat.2011.03.081

109. G.E. Stan, D.A. Marcov, I. Pasuk, F. Miculescu, S. Pina, and D.U. Tulyaganov, *Appl. Surf. Sci.*, **256**: 7102–7110 (2010); https://doi.org/10.1016/j.apsusc.2010.05.035
110. E.R. Urquia Edreira, J.G.C. Wolke, A.A. Aldosari, S.S. Al-Johany, S. Anil, and J.A. Jansen, *J. Biomed. Mater. Res. Pt. A*, **103**: 300–310 (2015).
111. A.R. Boyd, C. O'Kane, P. O'Hare, G.A. Burke, and B.J. Meenan, *J. Mater. Sci: Mater. Med.*, **24**: 2845–2861 (2013); https://doi.org/10.1007/s10856-013-5021-3
112. K. Takahashi, J.G.C. Wolke, T. Hayakawa, N. Nishiyama, and J.A. Jansen, *J.Biomed. Mater. Res.*, **84A**, No. 3: 682–690 (2008); https://doi.org/10.1002/jbm.a.31341
113. Y. Yonggang, J.G.C. Wolke, L. Yubao, and J.A. Jansen, *J. Mater. Sci.: Mater. Med.*, **18**: 1061–1069 (2007); https://doi.org/10.1007/s10856-007-0119-0
114. K. Ozeki, Y. Fukui, and H. Aoki, *Applied Surface Science*, **253**: 5040–5044 (2007); https://doi.org/10.1016/j.apsusc.2006.11.011
115. A.G. Solomenko, R.M. Balabai, T.M. Radchenko, and V.A. Tatarenko, *Prog. Phys. Met.*, **23**, No. 2: 147 (2022); https://doi.org/10.15407/ufm.23.02.147
116. P. Szroeder, I.Yu. Sagalianov, T.M. Radchenko, V.A. Tatarenko, Yu.I. Prylutskyy, and W. Strupiński, *Appl. Surf. Sci.*, **442**: 185 (2018); https://doi.org/10.1016/j.apsusc.2018.02.150
117. P. Szroeder, I. Sahalianov, T. Radchenko, V. Tatarenko, and Yu. Prylutskyy, *Optical Mater.*, **96**: 109284 (2019); https://doi.org/10.1016/j.optmat.2019.109284
118. O. Kolesnikova, N. Vasilyeva, A. Kolesnikov, and A. Zolkin, *Mining Inf. Anal. Bull.*, **10**: 103–115 (2022); https://doi.org/10.25018/0236_1493_2022_101_0_103
119. N.N. Zhanikulov, T.M. Khudyakova, B.T. Taimasov, B.K. Sarsenbayev, M.S. Dauletiarov, and R.O. Karshygayev, *Eurasian Chemico-Technological Journal*, **21**: 333–340 (2019).
120. N. Zhangabay, U. Suleimenov, A. Utelbayeva, K. Baibolov, K. Imanaliyev, A. Moldagaliyev, G. Karshyga, B. Duissenbekov, R. Fediuk, and M. Amran, *Buildings*, **12**: 1445 (2022); https://doi.org/10.3390/buildings12091445
121. V.G. Golubev, A.E. Filin, A.B. Agabekova, and T.K. Akilov, *Rasayan Journal of Chemistry*, **15**, No. 3: 1905–1915 (2022); https://doi.org/10.31788/RJC.2022.1536695
122. N. Zhangabay, B. Sapargaliyeva, A. Utelbayeva, Z. Aldiyarov, S. Dossybekov, E. Esimov, B. Duissenbekov, R. Fediuk, and N. Vatin, M. Yermakhanov, and S. Mussayeva, *Materials*, **15**: 4996 (2022); https://doi.org/10.3390/ma15144996
123. Q. He, L. Pan, Y. Wang, and F.C. Meldrum, *Cryst. Growth Des.*, **15**: 723 (2015); https://doi.org/10.1021/cg501515c
124. X. Meng, T.Y. Kwon, Y. Yang, J.L. Ong, and K.H. Kim, *Journal of Biomedical Materials Research. Part B: Applied Biomaterials*, **15**, No. 14: 373-377 (2006); https://doi.org/10.1002/jbm.b.30497
125. D.S. Gomes, A.M. Santos, G.A. Neves, and R.R. Menezes, *Ceramica*, 65, No. **374**: 282–302 (2019); https://doi.org/10.1590/0366-69132019653742706
126. S. Mahieu, P. Ghekiere, D. Depla, and R. De Gryse, *Thin Solid Films*, **515**:

1229–1249 (2006);
https://doi.org/10.1016/j.tsf.2006.06.027
127. J.A. Thornton, *Journal of Vacuum Science & Technology*, **11**: 666–670 (1974);
https://doi.org/10.1116/1.1312732

Received 27.06.2023;
in final version, 17.11.2023

А.Т. Турдалієв[1], *М.А. Латипова*[2], *Є.Н. Рєшоткіна*[3]
[1] Міжнародний транспортно-гуманітарний університет,
мікрорайон Жетісу 1, 32; 050063 Алмати, Казахстан
[2] Карагандинський індустріяльний університет,
пр. Республіки, 30; 101400 Темиртау, Казахстан
[3] АТ «АрселорМиттал Темиртау»,
пр. Республіки, 1; 101400 Темиртау, Казахстан

ПОКРИТТЯ НА ОСНОВІ СИНТЕТИЧНОГО ГІДРОКСИАПАТИТУ НА ПОВЕРХНІ УЛЬТРАДРІБНОЗЕРНИСТОГО ТИТАНУ ТА ЦИРКОНІЮ

Розроблення біосумісних матеріялів є мультидисциплінарним завданням і потребує взаємодії фізиків, хеміків, біологів, медиків, оскільки функціональна надійність матеріялів залежить від їхньої біохемічної, клітинної, тканинної та біомеханічної сумісностей. Цей напрям останніми роками інтенсивно розвивається; у результаті з'являється велика кількість дослідницьких статей. Передбачається, що склад біосумісного покриття нового покоління має максимально збігатися зі складом натуральної кістки людини та бути здатним імітувати кісткову тканину на своїй поверхні. В результаті наближення фазово-структурного стану та властивостей одержуваних покриттів на імплантатах до параметрів кісткової тканини можна досягти поліпшеної сумісности між ними. Під час формування біосумісних покриттів особлива увага приділяється створенню певного рельєфу (шерсткости) на поверхні імплантату. В даний час йде пошук нових технологічних рішень створення біосумісної шерсткої поверхні на імплантатах, що забезпечуватиме надійну інтеґрацію імплантату в кістковій тканині, оскільки наявні технології не задовольняють сучасним медичним вимогам.

Ключові слова: ультрадрібнозернистий матеріял, титан, цирконій, покриття, імплантат.